Dark Matter Searches at Colliders

Antonio Boveia,[1] Caterina Doglioni, [2]

[1]The Ohio State University, Physics Department, 191 W. Woodruff Avenue, Columbus, OH 43210, US
[2]Lund University, Fysikum, Division of Particle Physics, Professorgatan 1, 22363 Lund, Sweden

Xxxx. Xxx. Xxx. Xxx. YYYY. AA:1–29

https://doi.org/10.1146/((please add article doi))

Keywords

particle dark matter, invisible particles, weakly interacting massive particles (WIMPs), simplified models, colliders, LHC

Abstract

Colliders, one of the most successful tools of particle physics, have revealed much about SM matter. This review will sketch how colliders contribute to the search for particle dark matter, focusing on the highest-energy collider currently in operation, the Large Hadron Collider at CERN. Absent hints for the character of DM-SM interactions, it emphasizes what could be observed in the near future, the main experimental challenges presented, and how collider searches fit into the broader field. Finally, it underlines a few areas to watch for the future LHC program.

PARTICLE PROPERTIES OF DARK MATTER

Stability If DM is a particle, it does not seem to decay. Conservation laws, such as R-parity in Supersymmetry (SUSY) or a Z_2 symmetry, can prevent the DM particle from decaying into any lighter even-parity SM particle. Additionally, pairs of DM particles can be produced by the decay of other particles, charged under the same gauge group as the SM, or singly in the case the parent is a color triplet.

Darkness DM particles are effectively invisible to traditional collider experiments made of ordinary matter. However, the rest of the event is not. Invisible particles can be accompanied by one or more visible recoiling particles, leading to missing momentum in the transverse plane, whose magnitude is termed $\not{E}_T$. This is one of the main signatures of DM at colliders.

Contents

1. INTRODUCTION

Dark matter (DM) is perhaps the most persuasive experimental evidence for physics beyond the Standard Model of particle physics (1). If DM is indeed a particle (2), it has gravitational interactions with normal matter. It may have other, non-gravitational interactions, but these are relatively rare—dark matter is dark and has no electromagnetic charge. It is also stable, or at least it decays with a lifetime comparable to that of the universe. Finally, there is *a lot* of DM, about five times the standard matter (SM) described by the Standard Model of particle physics, with plenty of room to exceed the SM in its complexity. The current abundance of dark matter in the universe, derived from measurements of the Cosmic Microwave Background (3), is one of the few quantitative measures of DM, or indeed of any physics beyond the Standard Model (BSM). The main consequences of cosmological observations for particle dark matter are listed in the Sidebar.

The field of particle physics is increasingly keen to understand what Dark Matter (DM) is, if it is indeed a particle. Some experiments, termed Direct Detection (DD) experiments, look for galactic DM colliding with underground targets made of Standard Model matter (SM) (4). Others, termed Indirect Detection (ID) experiments, search for the products of annihilating dark matter concentrated within the gravitational potential wells of the Milky Way and elsewhere (5). None of these experiments has yet found conclusive evidence of DM. If the only interaction between DM and SM matter is gravitational, experiments will never see it. Yet the search for particle DM started relatively recently, and plenty of room for optimism remains.

Colliders, one of the most successful tools of particle physics, have revealed much about SM matter. This review will sketch how colliders contribute to the search for DM, focusing on the highest-energy collider currently in operation, the Large Hadron Collider at CERN. Absent hints for the character of DM-SM interactions, it emphasizes what could be observed in the near future, the main experimental challenges presented, and how collider searches fit into the broader field. Finally, it underlines a few areas to watch for the future LHC program.

2. REACTIONS FOR INVISIBLE PARTICLE SEARCHES AT THE LHC

DM produced at colliders would register just as neutrinos do, which is to say: not at all. In this chapter, we describe DM production from a pragmatic, collider physicist's perspective, focusing on a selection of simple models with distinct and testable LHC signatures[1] Moreover, we will use the term *invisible particles* rather than DM when emphasizing that detecting such particles need not be a discovery of DM[2].

The body of DM model literature can be divided into two extremes. Fully-realized, self-consistent models such as SUSY provide specific features that can be exploited for narrowly-targeted searches, while simplified models with a few ingredients can capture broad collider signatures of classes of models, serving as benchmarks for more general but less optimal searches. Key to both are the determinative details of the interactions between the DM and the SM, rather than the DM itself.

To restrict the scope of this review,

1. we describe only models where the DM interacts with SM hadrons, either directly or effectively;
2. we privilege models that include a Z_2 symmetry to stabilize DM;
3. we emphasize models connecting to a thermal, frozen-out relic; others, based on alternate cosmological histories (e.g. freeze-in), also have interesting LHC signatures (6)
4. we stress models employed for early LHC Run-2 searches, where the DM is a Dirac fermion, and the model mimics the pattern of flavor violation found in the SM (Minimal Flavor Violation, or MFV (7)).

Departures from these assumptions are discussed further in (8).

[1]For other perspectives, see the Reference Material.

[2]For example, invisible particles may decay after leaving the detector, a decay that is essential prompt on cosmological time scales.

2.1. Higgs and Z boson portals

Extending the SM with a single DM particle, and nothing else, one may arrive at portal models where the Z or Higgs boson mediates the DM–SM interaction. This is our first example of a *mediator*, a 'dark sector' particle that governs the DM-SM interaction. While the **Z portal** is perhaps the simplest model of DM that one can construct, LEP and direct detection experiments strongly constrain it, as discussed in Sec. 3.1 and in (9). **Higgs portal** models (10, 11) are more promising, as only the recent generations of collider and direct detection experiments has reached the energies and luminosities necessary to search for them. Direct collider searches for the invisibly-decaying Higgs bosons are augmented by measurements of other Higgs properties, which can be very sensitive to couplings to new particles.

The Z and Higgs portal models have relatively simple phenomenology. The mediators (the Z or Higgs boson) are light in comparison to the LHC energy and can be produced on-shell. Even if the invisible particles are much heavier, and invisible decays of the mediator are absent, collider searches may still study the Z and Higgs and constrain these models through their fully-visible decays.

2.2. Effective Field Theories and Simplified models of BSM mediators

One step further in complexity beyond the Z and Higgs portal models are models where the mediator is also a new particle, such as a heavier version of the Z boson (a Z') or an additional scalar.

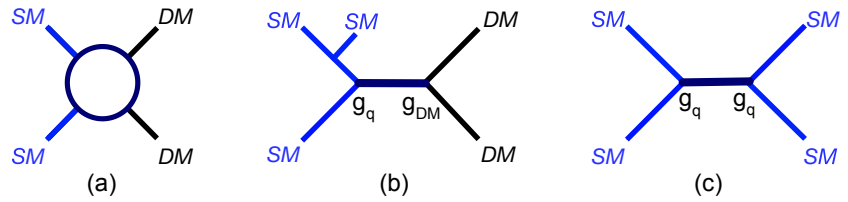

Figure 1

Sketches of (a) the DM–SM interaction in an effective field theory (EFT), (b) a corresponding simplified model mediated by a BSM particle (with additional radiation off one initial state quark) and (c) the same model where the mediator decays back into SM, with coupling constant for the mediator-quark-quark vertex, $g_{\rm q}$, and constant for the mediator-DM vertex, g_χ.

2.2.1. Effective Field Theories. In some situations, such as when a BSM mediator is heavy compared to the collision energy, the DM–SM interaction appears to be a contact interaction, with all observables completely determined by one rate parameter, the contact interacion scale, that controls the production rate, and a Lorentz structure choice, which has a modest effect on the transverse momentum distributions of the invisible particles. In this case, Effective Field Theories (EFTs) (12, 13, 14) provide a description of the production of invisible particles. A sketch of an EFT process is shown in panel (a) of Fig. 1. One may hope that such as description is sufficient for the LHC; the unknown high-energy details of

a complicated interaction are conveniently integrated out. Moreover, since EFTs do not fix a mediation mechanism, they provide a framework to systematically explore a wide range of possible physics.

If, instead, the interaction physics is kinematically accessible (e.g., the mediator mass is within reach of the typical momentum transfer in the collision), one should replace the EFT description with a model specifying further details of the SM–DM interactions (15). Without those details, however, one can still use the EFT language to provide results for later reinterpretation once a completion is known (16, 17).

2.2.2. Simplified models. When the collision energy is near or higher than the mediator mass, complementary avenues to study the mediating interaction develop, analogous to the transition from the Fermi model of weak interactions at low energies to the Standard Model at higher energies. For example, at the LHC, a heavy neutral Z′ mediator would often decay into the partons that produced it, and fully-reconstructing these visible decays can provide more information about the interaction than the invisible decays alone.

Under the reductionist assumption that only a few new particles will be important in the early phase of a discovery, simplified models can be developed for tree-level pair production of invisible particles (e.g. (18, 19)). The set of such models currently employed for ATLAS and CMS searches is described in Ref. (8), which builds upon much work from the wider dark matter community (e.g. (14, 20)) Though these simplified models must be embedded in a larger theory to satisfy theory constraints (21), they are sufficient to describe the leading order collider phenomenology in many cases.

The ATLAS/CMS Dark Matter Forum: provided reference implementations of the models in Ref. (8) at `https://gitlab.cern.ch/lhc-dmwg-material/model-repository` and are implemented in models for various event generators (e.g. DMSimp (22)).

The standard models include models with neutral mediator particles singly-produced at the LHC and decaying to pairs of invisible particles, and to pairs of SM particles (Figure 1 (b) and (c)). Two-body mediator decays are simple, attractive benchmarks. Colored mediators allow vertices involving only one DM particle and phenomenology akin to that of SUSY models with a squark mediator (23, 24, 25).

Models of BSM mediation can be classified according to the spin of the mediator: spin-1 vector or axial vector mediators (Z′), scalar mediators (termed ϕ in the following) and spin-2 mediators. Spin-2 mediator benchmarks have not yet been adopted by LHC searches; they produce diboson signatures not present in other models (26).

For additional decay signatures, for 'dark sectors' of many additional particles, and for far larger LHC datasets than at present, many more simplified models become interesting.

Massive color-neutral spin-1 bosons with vector or axial-vector couplings are nearly ubiquitous in BSM theories, so Z′ as the mediators connect with a wide class of models (15). Since the Z′ coupling to quarks must be non-zero for its production at the LHC, both invisible and dijet signatures are discovery channels. This coupling (or loop-level coupling) to SM partons is also required for nuclear recoils in underground DM searches.

The models in use at ATLAS and CMS contain either vector, axial-vector, or mixed couplings to quarks and a single species of invisible particle. The couplings of the Z′ (g_{q} to all quarks, g_{l} to leptons, and g_{χ} to invisible particles), the mass of the invisible particle m_{χ}, and the Z′ mass M_{med} are free parameters. Lepton decays, if not included explicitly at tree level, arise through the quark coupling at loop level (see Ref. (27) and references therein). Decays of the spin-1 mediator into neutrinos are also required by gauge invariance, and add an invisible decay channel that can enhance signatures of missing transverse momentum, depending on the size of the couplings (27). The spin structure of the Z′ couplings does not significantly change the LHC phenomenology, but has a much larger effect in signals in

non-collider searches.

Z′ mediated models can include additional couplings of the Z′ to acquire mass through a new baryonic Higgs h_B (28) that collapses to the simpler model above in the limit of very heavy Z′ mass. They can also be embedded in a Type-II Two-Higgs Doublet Model (2HDM) (28).

With certain values of the model parameters, especially low Z′ mass, the model can satisfy the relic density constraints (29). However, if taken in isolation, the model is non-renormalizable, and the axial-vector model violates perturbative unitarity in certain regions of the off-shell parameter space (29, 21, 30).

Color-neutral scalar and pseudoscalar bosons are an BSM analogue of the Higgs portal model. In comparison to the Z′ models, a BSM (pseudo-)scalar mediator model (31), has some additional peculiarities. Under MFV, the couplings of the (pseudo-)scalar bosons to fermions are mass-dependent. As with the Higgs boson, this has three familiar consequences: mediator production through loop-induced couplings to gluons (32) and associated with heavy flavor quarks (31); production cross-sections are smaller than for vector mediators; and visible decays of the mediator are dominantly to third generation quarks. Despite lower production cross-sections, the more specific experimental signatures allow for these models to be tested during LHC Run-2.

The (pseudo-)scalar models used by ATLAS and CMS are fully specified by the masses of the invisible particleand the mediator, the ϕ-invisible particlecoupling (g_χ), and the ϕ-fermion (g_q) coupling. Following the convention in (8), g_q is a pre-factor to the Yukawa couplings to fermions and set equal for all quarks. For the same model parameters, the scalar and pseudo-scalar models predict similar kinematic distributions.

When introducing an additional scalar, one must consider how the scalar relates to the Higgs boson. Large mixing with the Higgs can lead to strong constraints from Higgs measurements, for example when the scalar couples to DM through a Higgs portal (28). If the mediators are pure SM singlets, the model is not invariant under $SU(2)_L$ (33). To restore gauge invariance, mixing with the Higgs sector is crucial. Couplings to the electroweak gauge bosons can also be added as a consequence of electroweak symmetry breaking (34, 35). The tree-level signatures in this case include Higgs or vector bosons plus missing transverse momentum and, if the invisible particles are sufficiently light, invisible decays of the Higgs boson.

Colored scalar and pseudoscalar bosons allow direct coupling between SM carrying color and invisible particles carrying Z_2 charge (36, 23, 24, 25). Colored mediators can have a broader set of multi-jet signatures and kinematic features than the neutral mediator models, including the radiation of vector bosons by the mediator (25).

In colored (pseudo-)scalar models, the mediator must be heavier than the invisible particleto ensure invisible particlestability. For the current LHC results, the coupling, $g_{\chi q}$, between invisible particles and quarks, the invisible particlemass, and the mediator mass are free parameters.

The exchange of a scalar colored under SU(3) is analogous to squarks in the MSSM where only squarks and neutralinos are light. In the MSSM, the coupling between DM and the squark is constrained to be small(8). Without the requirements of a SUSY framework, this coupling need not be small. For example, if the DM is a standard thermal relic, the couplings required to obtain the correct dark matter density are generally higher than what used by SUSY models. Models with three generations of mediators can satisfy flavor constraints and the SM gauge symmetry (37).

2.2.3. Less simplified models. Simplified models can guide the design of generic searches but do not cover the full complexity of possible collider signatures that arise in more complete models. On the other hand, relying too heavily on a small sample of complete models risks focusing searches too narrowly on an unrepresentative set of signatures.

There are a large number of "less-simplified" models that attempt to find a middle ground between models that are too simplistic and those that are unnecessarily complex. Because the set of such models grows quickly with the number of ingredients, and there is not a broad consensus on which models should be a priority, very few of them have been explicitly considered by LHC searches. Here, we highlight a few such models with different signatures than the simplified models described above.

Co-annihilation models add two specifies of dark sector particle, one close in mass to the other. Examples can be found in Refs. (38, 39). The interaction between these two states drives the cosmological history (40), as processes involving both types of particles can efficiently annihilate into SM particles. The LHC signatures include missing transverse energy and multiple hadronic jets accompanied by multiple resonant or non-resonant hadronic jets, but can be very diverse, encompassing signatures typically found in wildly different BSM models (e.g., searches for lepto-quarks). In some cases, these signatures are untested by any current LHC search (38).

Most simplified models in use at the LHC assume MFV to ensure that the models are compatible with a vast and unwieldy assortment of experimental constraints on flavor-violating processes. Nevertheless, viable **non-minimal flavor-violating models** can be constructed, but one must then understand the impact of the many constraints (41). Mediators that couple to dark matter and a top quark are one category of flavor-violating model that remains least constrained by low-energy measurements (42). These yield a distinct 'mono-top' LHC signature.

Other **models with multiple mediators** with small couplings to SM particles have been developed to escape existing LHC constraints (43). The recent discovery of the Higgs boson places LHC at the forefront of the exploration of the SM scalar sector. Ultimately we don't yet know whether this scalar sector is limited to the SM Higgs boson. A single scalar mediator may not encode all important features of the more complicated phenomenology of more **complex scalar sectors**. Extended scalar sector models often involve signatures with $\not{E}_T$ accompanied by the Higgs or other SM bosons. One step beyond the simple scalar mediator model is to take mixing between this mediator and the SM Higgs boson, dictated by gauge invariance, into account (34, 28). A much larger step beyond this is to consider an extended Higgs sector such as a Two-Higgs Doublet Model (2HDM) where one or more of the scalars acts as the SM-DM mediator (44, 45, 33). In these models, the new mediator mixes with the Higgs partners rather than with the SM Higgs, so that the model remains compatible with Higgs measurements. Some models developed for LHC searches focus on one Yukawa structure (Type-II). The particle content includes two CP-even bosons (one of which is the SM Higgs boson), two CP-odd bosons (of which one is the pseudoscalar DM mediator), two charged Higgs bosons, and the invisible particle. Masses and couplings of these models are chosen to respect vacuum stability (45), electroweak and flavour constraints, and to reproduce the observed dark matter abundance.

2.3. Supersymmetric models and other complete theories

So far, we have considered rather general simplified models inspired by interactions found in the SM. These are obviously far from all the possibilities. Further sources of inspiration for searches are the large number of BSM theories that have been developed to solve theoretical problems of the SM, and the mechanisms through which these provide invisible particles.

Superymmetry (SUSY) is one class of such theories, postulating partner particles to all SM degrees of freedom to stabilize the mass of a light Higgs boson. Reviews of supersymmetric DM models can be found in (46). Instead, we will broadly sketch models relevant to recent experimental progress and stress where we expect future developments.

Supersymmetric relic dark matter, the archetype for the WIMP idea, has a long history (47). Of these, the most viable and well-studied has been neutralino dark matter. The neutralino, a spin 1/2 partner particle to the SM gauge bosons, is often assumed to be the lightest supersymmetric particle (LSP). R-parity conservation makes the LSP stable (48) and prevents proton decay.

In the Minimal Supersymmetric extension of the Standard Model (MSSM), there are four neutralinos, each a mixture of SM boson superpartners: a wino, a bino, and two higgsino fermion states. The lightest neutralino may be called 'bino-like,' 'wino-like,' or 'higgsino-like' in regions of MSSM parameter space where one of these components dominates the mixture. The phenomenology of these is different from most of the simplified models in the previous section, and it depends on mixture and on the particle spectrum. The LHC signatures feature missing transverse momentum from the neutralino and a high multiplicity of other objects (leptons, jets) produced in cascade decays of heavier superpartners.

The MSSM is a complete theory with more than 100 independent parameters, but realistic SUSY models might be far simpler.Such models are used as predictive benchmarks for DM searches. One of these is the phenomenological MSSM (pMSSM), which assumes no sources of CP violation beyond the SM nor Flavour-Changing Neutral Currents, and retains universal couplings and masses for first and second generation superpartners, reducing the number of MSSM parameters to 19.

Another DM candidate in gauge- or gravity-mediated supersymmetric models is the gravitino, a 3/2-spin particle superpartner of the graviton. Gravitino interactions are suppressed by the Planck scale (10^{18} GeV) before SUSY breaking. This has consequences both on their viability as a thermal relic and on their phenomenology. In gauge-mediated SUSY, the gravitino can be a DM candidate for a non-standard cosmological history (49). Similar to the neutralino case, the identity and masses of heavier states decaying to the gravitino LSP determine its phenomenology. However, the gravitino interactions are very weak, posing problems for direct and indirect detection searches.

Because of the huge variety of potential experimental signatures, SUSY searches also often adopt a simplified model approach, decoupling the particles that determine the lowest energy collider phenomenology (generally LSP and NLSP) from the rest of a heavier particle spectrum (19). As in the general simplified models described earlier, extending the MSSM quickly generates a plethora of non-minimal possibilities.

2.4. Long-lived particle models

Another class of models found within and beyond SUSY are models feature suppressed cascade decays of a heavier particle (the NLSP in SUSY) to a lighter particle (the DM LSP

in SUSY). The suppression can be so large that the particle travels a macroscopic length within the detector before it decays. Within SUSY, one way to achieve this suppression is for the NLSP to decay through a heavy intermediary. Split supersymmetry models are a subset of SUSY models where the gluino must decay through a heavy, off-shell squark (50). The heavier the mass of the squark, the longer-lived the gluino. Alternatively, the NLSP decay can be heavily suppressed by some power of the mass difference with the LSP. This mass difference also affects DM co-annihilation rates and therefore the DM abundance (40). Finally, another way to achieve long-lived decays is with parameterically small couplings, as in the case of gauge-mediated supersymmetry models where the long-lived NLSP decays to its SM partner plus the gravitino (49), with a SM analogue in the Cabibbo-suppressed B-meson decays. Because of the prevalence of these mechanisms, it is important to look for long-lived cascade decays.

Besides SUSY, one can find long-lived signatures within the generic simplified models in Sec. 2.2.2 for small enough couplings. If one assumes thermal freeze out, the coupling of the mediator to DM pairs is bounded from below to obtain a sufficiently large annihilation cross section. However, it's anybody's guess what mechanism in the early universe was responsible for the observed DM density. In alternate scenarios, such as "dark freeze out" where DM can annihilate directly to BSM mediators but not viceversa, the mediator couplings to the SM can be far smaller than allowed in standard thermal freeze out (51, 52). The freeze-in scenario (53, 6) is another possibility for very weak DM–SM interactions. Despite such small couplings, a sufficiently light mediator can be produced at colliders with appreciable cross section. Many models have been proposed in this direction. For example, DM can interact with the SM via a dark vector boson of a U(1)' dark symmetry, equivalent to the SM's U(1) but with much smaller couplings (54), such as those originated by kinetic mixing. The mediator can also be a dark scalar boson (a "dark Higgs") that only couples to the SM, akin to a Higgs portal (55). In both cases, the dark boson mediator can be light and long-lived (51), and its visible decays into SM particles or associated production with a SM boson provide the main collider handle for observation (55). These scenarios can also be probed by complementary beam dump and fixed target experiments (56). Simplified co-annihilation models with long-lived particles have also been proposed (57).

2.5. Dark interactions

In the above, we've sketched some of the models and signatures that are currently being sought at colliders. Next, we review experimental searches for invisible particles, in light of the models discussed above. Nevertheless, we have left many models uncovered. From one point of view, any model containing stable particles interacting feebly with the SM is a theory of DM. Drawing the connections between this model and astrophysical DM is challenging, but this is the key difference between models of DM and other models of BSM physics.

The dark sector can be arbitrarily complex, as long as the particles and interactions it contains satisfy cosmological observations (58, 59). The models listed above are simple examples of such dark sectors, where the mediator particles (e.g. dark bosons) provide the connection with the SM. Many other models are worthy of mention here, including asymmetric DM models, where dark sector particles and antiparticles are not produced in equal amount, in the same fashion as matter and antimatter for SM baryons (60), and models of "neutral naturalness" realizing a mirror copy of the SM without any low-mass

equivalent of the SUSY colored partners (61).

3. EXPERIMENTAL RESULTS

The interactions described in the previous chapter have many consequences in astrophysics (where they could modify the DM density) and in collider and non-collider particle physics experiments.

Collisions of known particles at high energy, observed with well-understood detectors, have been a very successful tool, leading to the discovery of many of the fundamental components of known matter in the SM. While collider experiments alone cannot discover DM, they can discover invisible particles, and this could open up direct study of DM–SM mediators in other channels and of additional particles in a dark sector. DM–SM interactions may be feeble because they are mediated by a heavy mediator or by a mediator with small couplings to SM. High energy and large numbers of collisions are needed to probe for these interactions, and the LHC, which presently collides protons at a center-of-mass energy of 13 TeV, will deliver both in the coming years.

Below we discuss experimental searches for invisible particles from three LHC (62) experiments, ATLAS, CMS, and LHCb (63, 64, 65) and briefly touch on some results from previous colliders. The LHC results include up to 36 fb^{-1} of proton-proton data taken through 2017 during Run-2, more than three times what used for the Higgs discovery, but only 1% of the data expected during the full High Luminosity (HL-LHC) run.

For signature, we outline how the relevant searches are done, some the challenges, and the information they provide on the properties of hypothetical particles (couplings, mediator mass, other parameters of the Lagrangian in a particular model). In a later chapter, we describe how collider information can be related to non-collider DM searches and to the present DM abundance, such as how conclusions drawn from relativistic collisions can be extrapolated to the non-relativistic collisions of DM+nucleons.

Run-1: First period of LHC running (2010-2012) at 7 and 8 TeV center-of-mass energy, where approximately 20 fb^{-1} of data were collected by ATLAS and CMS.

Run-2: Second, ongoing period of LHC running (2015-2018) at 13 TeV center-of-mass energy, planning to collect approximately 100 fb^{-1} of data.

HL-LHC: High-Luminosity LHC running period, planned to start in 2026 to collect 3000 fb^{-1}.

3.1. Searches for invisible particles production mediated by SM-bosons

For copious production of low-mass invisible particles, colliders already provide spectacular evidence: the huge rate of neutrino production mediated by the W and Z bosons. Neutrino production via the Z boson is often the largest background to searches for new invisible particles and is important to understand well. The rate of would differ from the SM prediction if the Z boson is coupled to additional invisible particles lighter than about half its mass. The most precise measurement of the invisible Z width, 499.1 $\pm$ 1.5 MeV, has been inferred from the total width at LEP (66). This can be used to constrain the parameters of models such as Z portals (67, 9). The coupling between the Z and an invisible Dirac fermion is constrained to be smaller than 2-3% for invisible particles that are significantly lighter than half the Z mass. A less-precise direct measurement of the Z's invisible width, also by LEP, uses invisible decays with a photon emitted as initial state radiation (ISR), selecting events with a single photon, the total invisible transverse momentum inferred from momentum balance with the visible particles ($\not{E}_T$), and little other event activity. This $\not{E}_T$ +ISR has become a key signature for invisible particle searches at colliders. At the LHC, precision measurements continue to test the production and decay of Z bosons for the effects of invisible particles. For example, ATLAS has measured the ratio of cross sections for jet and $\not{E}_T$ production, dominated by invisibly-decaying Z bosons, to production of Z

MEASURING INVISIBLE PARTICLES: $\not{E}_T$ RECONSTRUCTION

Precise measurements throughout each detector systems are crucial to measure $\not{E}_T$ in experiments at hadron colliders, as its calculation should include all particles in the event. Contributions that are not attributed to physics objects form the soft component of the $\not{E}_T$ (73, 74). One of the main challenges for $\not{E}_T$ measurements is excluding contributions from additional proton-proton interactions whose debris are detected at nearly the same time as the hard scatter (pile-up). Searches for invisible particles also need to reject events with large $\not{E}_T$ if the visible energy is due to non-collision backgrounds.

Challenge: pile-up in $\not{E}_T$ reconstruction. In addition to suppressing pile-up suppression within the calorimeters, tracking information can be used to determine whether energy deposits originate from the primary collision vertex. The combination of this information is used to remove pile-up both in the physics objects used for $\not{E}_T$ calculation and in the overall event energy balance (74, 75).

Challenge: fake $\not{E}_T$ rejection. Non-collision backgrounds, such as cosmic rays, beam background and detector noise have a significant contribution to the tails of the $\not{E}_T$ spectrum, as shown in Fig. 2 Specific quality cuts, based on the presence of tracks associated to the deposited energy and on energy deposited in the various calorimeter layers are applied to reject these events (76). The number of events passing the jet+$\not{E}_T$ analysis selection before these quality cuts is about ten times larger than the SM contribution (77).

bosons decaying to dilepton pairs, a ratio which is sensitive to the production of additional invisible particles (68).

The Z boson is also key to invisible decays of the newly-discovered Higgs boson. Higgs decays to neutrinos contribute to less than 0.1% of its total decay width in the SM, proceeding through a pair of Z bosons that then both decay invisibly. With present data, this rate could become observable if the Higgs is coupled to additional invisible particles (69, 70). To constrain the invisible width of the Higgs, ATLAS and CMS cannot directly measure its total width in a model-independent fashion (71). Searches instead attempt to directly observe these decays via their recoil against visible particles (substantial $\not{E}_T$), or by comparing measurements of the Higgs parameters under additional assumptions about the BSM physics. Direct Higgs to invisible searches have used Run-1 and Run-2 data, combining several strong and electroweak production channels. Combining direct and indirect searches, the most stringent bound on the fraction of invisible decays of the Higgs boson is 23% (72, 70). This places constraints on Higgs portal couplings of 1-2% for Dirac invisible particles much lighter than half the Higgs mass.

3.2. Generic searches for invisible particles from BSM mediation

Searches for invisible decays via SM mediators (the Z or Higgs) can be viewed as special cases of searches for more general BSM mediation of invisible particles. Since mediator decays to invisible particles are suppressed if the invisible particlemass is heavier than half the mediator mass, the fixed masses of SM mediators place a ~ 45 –65 GeV upper bound on the invisible particlemass that can be observed. Moreover, the distribution of $\not{E}_T$ in such events has a similar shape to that of the Z-mediated neutrino background.

For heavier BSM mediators, this is not necessarily the case. Their decay to invisible particles can produce $\not{E}_T$ distributions substantially different than the SM background.

The complexity of the processes mediating invisible particle production determines the composition of the visible recoil, and so searches are employed across many different visible particle signatures. Nevertheless, many collider searches, from LEP to Tevatron to the most recent LHC searches (e.g. (78, 13)), aim to be model-agnostic, designed to detect an excess of $\not{E}_T$ over the SM background with minimal assumptions about the visible objects in the recoil. Selecting events (triggering) in a model-agnostic way can often be done by looking for substantial $\not{E}_T$, but for models that do not produce large $\not{E}_T$, one is forced to assume more about the visible recoil. We start with the 'jet+$\not{E}_T$' search, which illustrates techniques used in other general invisible particle searches, and shares with them many of the same challenges. Traditionally, these have been called 'mono-X' searches, but the radiation of a single object is only the leading process in the simplest reactions (79).

A *trigger:* selects which LHC collisions are recorded for analysis. For descriptions of the ATLAS and CMS triggers, see (80).

3.2.1. Searches with jets. One way to reduce the model dependence of the searches is to require that the recoiling visible particles are produced by SM processes, not in the dark interaction. ISR meets this criteria. SM bosons are likely to be present in any BSM process, radiated from initial state partons at rates fixed by the SM. Because gluon ISR is far more prevalent than the other forms, the jet+$\not{E}_T$ search is a key search in this approach.

A LHC jet+$\not{E}_T$ search (81, 82) typically selects collision events with a moderate amount of $\not{E}_T$ (in the 13 TeV analyses, typically above 200 GeV, sufficient to record such events at a manageable rate) and at least one jet with transverse momentum, p_{T}, larger than 100-200 GeV in the central region of the detector ($\eta < 2.4$). From this sample, further restrictions on additional hadronic jets and other visible particles are used to suppress contributions from SM processes and from instrumental backgrounds causing spurious $\not{E}_T$. These requirements reduce the generality of the analysis but also better isolate signal-like events. For example, contributions from W bosons decaying to leptons are reduced by vetoing events with leptons, and top pair production is reduced by limiting the number of jets present. The remaining SM multi-jet processes can exhibit large $\not{E}_T$ when one or more jets is mismeasured. Such mismeasurements often result in $\not{E}_T$ along the axis of a jet, and this feature is used to reduce the background to about 1% of the total. Non-collision events (e.g., intersecting cosmic rays, beam-gas interactions, and calorimeter problems) can also produce spurious $\not{E}_T$ events. Fig. 2 shows that such events dominates a high $\not{E}_T$ data sample unless rejected with criteria tailored to the expected collision time and detector hardware.

Signal region: a population of events enriched in contributions from signal processes. Data in this region are compared to SM predictions to search for new processes.

Control region: a population depleted of signal contributions but with other characteristics close to the signal region. Control data are used to model or validate SM predictions.

After the above criteria, one arrives at a sample composed mainly of invisible decays of the Z boson (approximately 55-70% of the total background). A substantial rate of semi-leptonic decays of the W boson also survives the lepton veto when the lepton is not reconstructed (approximately 20-35% of the total background.

The main observable is typically the number of events in one or more $\not{E}_T$ *signal regions*, either exclusive (in bins of $\not{E}_T$) or inclusive (considering all events above a given $\not{E}_T$ threshold).

Because invisible particles have feeble interactions with the colliding partons, and thus low production cross sections, these searches need very precises estimate of the shapes of the backgrounds. A background estimate solely from MC simulation is subject to uncertainties on both theory and detector simulation affecting the total cross-sections and is therefore not precise enough. To estimate the Z- and W-mediated neutrino backgrounds, recent ATLAS and CMS searches combine the information from data, in signal-free *control regions* selecting visible boson+jet processes (W, Z, γ) and the most recent perturbative calculations (83), much more precise estimates. Backgrounds from top processes in ATLAS are estimated

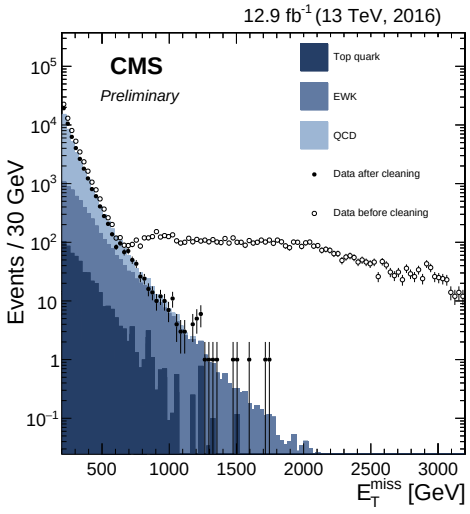

Figure 2

The $\not{E}_T$ distribution of events, selected for high total hadronic energy and at least two jets with $p_{\mathrm{T}} > 400$ and 200 GeV, before (open circles) and after (filled circles) rejecting spurious $\not{E}_T$ backgrounds (74). The predictions of MC simulations (shaded) are also shown. Strong non-collision background suppression is vital to $\not{E}_T$ +X analyses.

using a control region with $b-$jets, while CMS takes this background from simulation. Estimates of smaller backgrounds rely more heavily on simulation.

To date, precision achieved for the background estimate is 2–7% (CMS) and 2–10% (ATLAS), depending on the $\not{E}_T$ range. The remaining uncertainties mainly arise from the identification of leptons (CMS) and the understanding of the jet and $\not{E}_T$ calibration (ATLAS).

With no excesses observed, these searches can set 95% CL limits on the production cross-section of invisible particles, typically spanning from 0.5 pb to 2 fb depending on the $\not{E}_T$ threshold (81). ATLAS and CMS also report constraints on a selection of mediator models. These constraints can be interpreted as limits on the interactions between the mediator and the SM (e.g.g_{q}) under specific sets of model assumptions, not on the mass and other properties of the invisible particles per se. As an example, for the simplified model with (axial-)vector mediators, mediator masses of up to 1.5–1.9 TeV (81, 82) are ruled out for an invisible coupling of g_χ =1. For lighter mediators than this bound, the search can exclude SM couplings of order 0.1, or alternatively lower g_χ values than unity. With this amount of data, the searches are also becoming sensitive to lower-rate interactions mediated by (pseudo-)scalar mediators, and a recent ATLAS search (81) sets explicit constraints on colored scalar mediators, where, for unit couplings and invisible particle masses of up to 100 GeV, the mass of the mediator is constrained to be above 1.7 TeV. Jet+$\not{E}_T$ results from LHC Run-1 and the Tevatron have also reported constraints on EFT models.

Since this type of searches can constrain a wider variety of interactions than explicitly considered, steps have been taken to allow easy reinterpretation of the results. ATLAS and CMS provide more detailed experimental results on the HEPData platform (84). CMS also provides a simplified likelihood function encapsulating the result (85, 82).

3.2.2. Searches with photons and vector bosons. Besides gluons, other particles can constitute visible-particle recoil. In models where the recoil must arise from ISR, the rates for photon and electroweak boson radiation are much smaller than for gluon radiation. Nevertheless, searches in $\not{E}_T$ +photon and $\not{E}_T$ +Z channels can play a complementary role alongside jet+$\not{E}_T$, with a smaller and different mix of backgrounds and different systematic uncertainties. ATLAS and CMS have both performed searches in each channel. With lower backgrounds, events can be recorded with lower kinematic thresholds, resulting in lower MET and visible p_{T} selections. For example, the lowest $\not{E}_T$ value probed by the Z+$\not{E}_T$ search, where the Z decays into leptons (86, 87), is around 100 GeV, vs. 200 GeV for the jet+$\not{E}_T$ search (82).

These searches can play a much more powerful role when the recoil arises from the dark interaction itself rather than ISR. In these cases, photon or vector boson recoil (e.g. (88, 89)), rather than gluon recoil, may be the dominant signature. In these searches, the event selection and the background estimation strategies generally mirror those of the jet+$\not{E}_T$ search, but vary with the type of recoil, taking advantage of the special features of the signal. In the photon+$\not{E}_T$ searches (90, 91), components of hadronic showers mis-identified as isolated photons are a sizable background to be rejected. The searches with electroweak bosons decaying hadronically use jet substructure techniques (82, 92) to recover information about boson mass and decay in events where the decay products from the high-p_{T} boson are collimated. QCD jets will not present any substructure (93), while the decay products of vector bosons grouped into large-radius jets have a typical two-prong pattern from the hadronization of the quark-antiquark pair.

None of these searches yet observes a signal. The searches are not in general as sensitive as the jet+$\not{E}_T$ search to models where the visible recoil arises from ISR, because of smaller signal acceptance and comparable signal to background ratio, but they can be remarkably competitive—after the jet+$\not{E}_T$ searches, the photon+$\not{E}_T$ searches are the next-to-most powerful probe. However, these searches provide the most stringent limits on some models where the boson in question is directly involved in the dark interaction (28).

3.2.3. Search signatures including the Higgs boson. One can also look for the newly-discovered Higgs boson in the recoil, but due to the heavy mass of the Higgs and the small heavy-flavor content of the proton, the rate of Higgs ISR is insignificant. Thus, searches for $\not{E}_T$ +Higgs target dark interactions in which the Higgs is a direct participant, and therefore the interaction is closely tied to the Higgs sector. This is a feature of many models that extend the SM scalar sector.

Dedicated searches for $\not{E}_T$ +Higgs select Higgs events similar to the inclusive Higgs measurements, then require substantial $\not{E}_T$ to reduce the backgrounds to the search. In the Run-2 data, searches in the $H \to \gamma\gamma$ (94, 95) and $H \to b\bar{b}$ (96) channels have been performed. Searches in the ZZ, WW and $\tau\tau$ channels are expected to contribute as well, once substantially more data is collected.

The $\not{E}_T$ $+H \to \gamma\gamma$ searches (94, 95) benefit from their ability to precisely constrain the diphoton pair to the Higgs boson mass. They are still statistically-limited. The relatively low backgrounds allow probing for anomalous $\not{E}_T$ as low as 50 GeV (94) . The diphoton invariant mass is fitted in different signal categories, each optimized for different types of signal models. The search for Higgs decaying to two bottom quarks (96) requires $\not{E}_T$ >150 GeV. All backgrounds except for the QCD background are estimated using MC simulation and constrained in dedicated control regions. It also employs jet substructure techniques

for $\not{E}_T$ >500 GeV to select boosted Higgs decays from a background of QCD processes. The main systematic uncertainty for the lower $\not{E}_T$ signal region is the modelling of the V+jets background, while higher $\not{E}_T$ signal region is still statistically limited with the current dataset.

Absent signal, limits are set on the baryonic Higgs benchmark model outlined in Sec. 2.2.2 with g_q =1, g_χ =1, $g_{hZ'Z'}/m_Z$=1, $sin(\theta_B$ =0.3, and on a Z'-2HDM models [3].

Higgs+$\not{E}_T$ and Z+$\not{E}_T$ searches are also sensitive to extended scalar sectors such as two Higgs doublets with a scalar or pseudoscalar mediator (44, 45, 33).

3.2.4. Searches with third-generation quarks. In scalar- and pseudo-scalar-mediated simplified models, one can exploit the production mechanism in the search design. For instance, the mediator can be produced along with two top or bottom quarks, leading to a signature of $\not{E}_T$ and multiple b-jets.

A recent ATLAS search in these channel (97) is optimized for both recoil consisting of semileptonic and fully hadronic top quark decays and recoil with one or two bottom quarks. This signature is similar to that of third-generation quark superpartners and can be part of dedicated SUSY searches or used for reinterpretation (98, 99). SUSY searches suppress most of the $t\bar{t}$ background, matching specific models to specific, low-background signal regions. Relative to these approaches, the search in Ref. (97) is less narrowly targeted at specific models, where control regions can be more reliably developed, instead relying more heavily on simulation. The sensitivity of searches of $\not{E}_T$ associated to top quarks is comparable for the two strategies.

No excess is observed in any of these searches. For invisible particlemasses of 1 GeV, color-neutral pseudo-scalar mediators of mass 20-50 GeV (98) and scalar mediators of masses up to 100 GeV (99) are excluded. Signatures with $b\bar{b}$ pairs are less sensitive to models that do not explicitly privilege bottom quarks, but can set much higher limits on colored mediator masses in case of preferential couplings to bottom quarks (100).

Other LHC searches in this category are those only including only one top or bottom quark (also called mono-top or mono-bottom searches) (101, 102). They place constraints on models that include singly-produced invisible particles through flavor-changing neutral currents (42).

3.3. Searches for SUSY invisible particles

So far, motivated by simple models, the $\not{E}_T$ +X experimental searches discussed make few choices about the visible recoil particles, i.e. the species of a single particle, yet these already lead to a plethora of diverse signatures.

Models with more degrees of freedom may vastly expand the set of signatures to be explored. Supersymmetry (SUSY) adds, along with invisible particles, many more ingredients: a full copy of the SM particle spectrum. Each superpartner features particular decay chains that can be targeted to a greater or lesser degree, privileging either generality or maximal sensitivity. Compared to the generic searches above, SUSY searches general opt for a more specific decay topology and thus apply more stringent event selections based on the expected kinematic features, often using discriminating variables based on a combined

[3]In the case of the Z'-2HDM particles model, CMS and ATLAS set different masses for the new Higgs bosons, so the constraints are not yet directly comparable.

mass of visible and invisible particles (see e.g. (103)) to recover the ability to resolve various resonant decays.

SUSY has received much attention by ATLAS and CMS, and many searches for its particles, such as for squarks and gluinos, have a long history at earlier coliders as well. In this section, we give a flavor of experimental results of more recent interest.

No SUSY search so far has produced a conclusive signal. However, given its multifarious signatures, it's difficult to make general statements about the current status, even for simplified models of SUSY. Perhaps the best one can say is that searches for strongly-produced superpartners constrain them for masses approaching a couple of TeV (see Fig. 3 and e.g. (104, 105)), for neutralino masses up to a TeV, and, on the other hand, other processes are less constrained. Direct production of weakly-coupled superpartners has a much smaller production rate, and hence the constraints on them are significantly weaker. Third-generation squarks are generally only constrained to be at least several hundred GeV for neutralinos of similar masses, see e.g. (106, 107). But there are numerous exceptions to these blanket statements, even before one remembers that the masses exclusions shown in the figure only apply to specific slices of a multi-dimensional model parameter space.

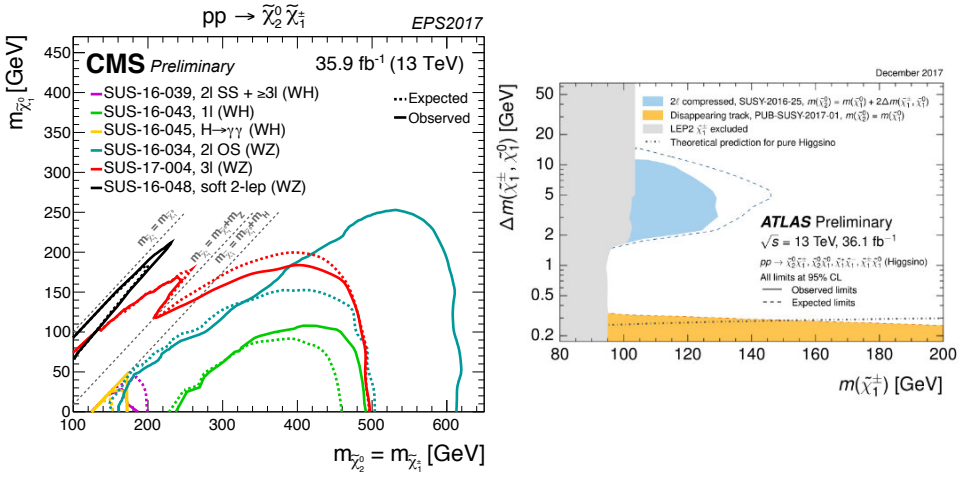

Figure 3

Mass reach of ATLAS and CMS searches for a selection of results targeting electroweak SUSY production, available as of December 2017. From (108, 109).

Though LHC searches have mainly probed strongly-produced SUSY channels so far, searches for rare processes are now entering their prime. With the data now collected, one can explore the electroweakino parameter space (see e.g. (110, 111)). Searches for gauge boson superpartners (gauginos) can reach approximately 1 TeV if the superpartners of SM leptons are light, and the search can benefit from a high leptonic branching ratio, whereas their reach is lower if their decays proceed through W and Z bosons. More luminosity also provides access to new regions of parameter space for specific signatures, e.g. "compressed" regions where small mass differences between superpartners lead the signals to lie buried in large backgrounds at low $\not{E}_T$ (112, 113). Small mass differences can also suppress super-

partner decays, resulting in long lifetimes. This can be exploited to study regions with a mass difference as low as 0.2 GeV for Higgsino models (114). Other mechanisms of decay suppression can do this as well (e.g. split SUSY (115)).

Despite the unwieldy diversity SUSY signatures, a sufficiently specific model can provide a concrete framework on which to build an understanding of the combined effect of many experimental constraints. Ref.(116), continued in LHC experiments (117, 118), uses the pMSSM to define a finite (though large) parameter space for whichthe wealth of experimental constraints can be systematically evaluated. Though this approach is not exhaustive, it can identify under-examined signatures for future emphasis. Besides particle physics data, one may also identify the LSP with astrophysical DM to focus more specifically on regions compatible with a given cosmology, as in Ref. (107).

Collaborations such as GAMBIT (119) and Mastercode (120) have combined a variety of tools to aid in such efforts. These codes encapsulate search results in statistical outputs which can be combined to construct global constraints for the models of interest. For example, one may compile the likelihood functions for the parameters of a SUSY model given the results from collider, direct, and indirect detection experiments.

3.4. Searches in association with long-lived particles

Prompt decays produce visible recoil originating at the collision point, and thus it can be reconstructed using the techniques for which the experiments were designed. The long-lived mediators described in Chapter 2.4 present different experimental challenges. For short lifetimes, long-lived particles (LLPs) can decay inside the tracking detectors, appearing as displaced decay vertices. Some SUSY decay chains lead to disappearing tracks, if the visible particles decay into the LSP and soft particles (see e.g. (121, 122)). Even longer-lived particles can decay in the calorimeters or in the muon spectrometers or they may even exit the detector cavern completely before decaying. These complications add yet another dimension of complexity to such searches, because observing the events may require dedicated triggers, reconstruction algorithms, and even detectors(123, 124).

Searches at colliders use a variety of experimental signatures to target different types of dark bosons, such as dark vector or scalar bosons. An LHCb search for dimuon resonances (125) is sensitive to visible decays of vector mediators in the mass range between 10 and 70 GeV. This search can use the entire sample of dimuon decays delivered to LHCb, recorded at the full collision rate directly at the trigger level (126). Below 10 GeV, experiments at electron-positron colliders have searched for dilepton resonances or missing mass produced in association with ISR photons (see e.g. (127, 128)). LHCb also searches dimuon events for scalar bosons with masses between 250 MeV and 4.7 GeV (129), for a range of lifetimes. Dark bosons can also arise in Higgs decays via a hidden-sector mechanism. For example, the searches in (130, 131) look for exotic Higgs decays into collimated "lepton-jets', constraining the decay rate to be below 10% for a range of dark photon lifetimes. Ref. (55) provides a review of many possibilities.

3.5. Consequences of neutral-mediated models: visible decays

Dark interactions might also be probed without actually producing invisible particles. For example, if the mediator particle can be produced via interactions with quarks, it may also decay into quarks. In this case, dijet and top-top resonance searches (see e.g. (132, 29)) can constrain it.

CHALLENGES FOR TRIGGERING AT HADRON COLLIDERS

The LHC collides protons every 25 ns in nominal conditions. The decision to record collision events for further analysis is made by the trigger system (80, 136, 137). Its first hardware-based level uses partial detector information for fast decisions. Its second software-based level uses more refined algorithms and has access to further detector information.

Triggering on low-p_{T} objects The trigger system records events above a certain threshold (e.g. leading jet p_{T} or event $\not{E}_T$), since energetic processes are likely to contain interesting features. Only a small fraction of events below these thresholds is recorded, penalizing signals with lower-energy signatures. However, if only final-state objects reconstructed by the trigger system are recorded, instead of full event information, the storage limitations can be overcome (126, 134, 136).

***Pile-up* in trigger** Pile-up can add energy uncorrelated to the hard process of interest, increasing the event rate for a given trigger threshold: trigger $\not{E}_T$ rates grow exponentially with the number of additional interactions. For this reason, increases in LHC instantaneous luminosity and dataset size come at the cost of increased thresholds. Dedicated pile-up suppression algorithms including partial tracking information are used in the trigger reconstruction (138, 75). ATLAS and CMS foresee dedicated hardware systems to obtain full tracking information in future LHC runs (139, 140).

Dijet resonance searches have been used routinely at hadron colliders to probe for new particles at newly-reached collision energies. They exploit an expected absence of features in the dijet invariant mass distribution to estimate the search background directly from a fit to the data, minimizing modelling and theory uncertainties. This permits the observation of low-rate localized excesses (width/mass up to $\sim 15\%$) from resonant dijet production (133, 134). For wider signals, searches exploiting the scattering angle of dijet events can be used (135, 133).

At the LHC, typical dijet searches lose sensitivity at masses below about 1 TeV (141, 142), where high rates force the experiments to discard a large fraction of the data in the trigger. Some challenges of triggering are discussed in the Sidebar. One can reduce this threshold to 400 GeV (134, 143) by recording much less information for these low-mass events (126, 134, 136). Alternatively, one can look at the subset of dijet events where a high-p_{T} ISR object happens to trigger (144, 145). Even lower mediator masses can be reached exploiting substructure techniques when the mediator decays are collimated into a single jet (145, 146). Dedicated searches for resonances of third-generation quarks (147, 148, 149) are also performed.

Dilepton resonance searches also constrain mediator couplings to leptons (150, 151). For dielectron and dimuon searches, the main backgrounds arise from Drell-Yan processes. These are estimated with simulation corrected for NNLO effects and normalized to the Z boson yield in data.

Fig.4 illustrates constraints from the dijet resonance searches mentioned above, on the quark coupling of the mediator in an axial-vector simplified model, as a function of the mediator mass, for a model that assumes no tree-level couplings to leptons and no possible decay to DM. Searches for boosted mediator decays are sensitive to masses as low as 50 GeV and quark couplings g_{q} as low as 0.06 at 60 GeV. Jets from the mediator decay are spatially separated for mediator masses above 250-300 GeV, where the γ and gluon ISR + dijet

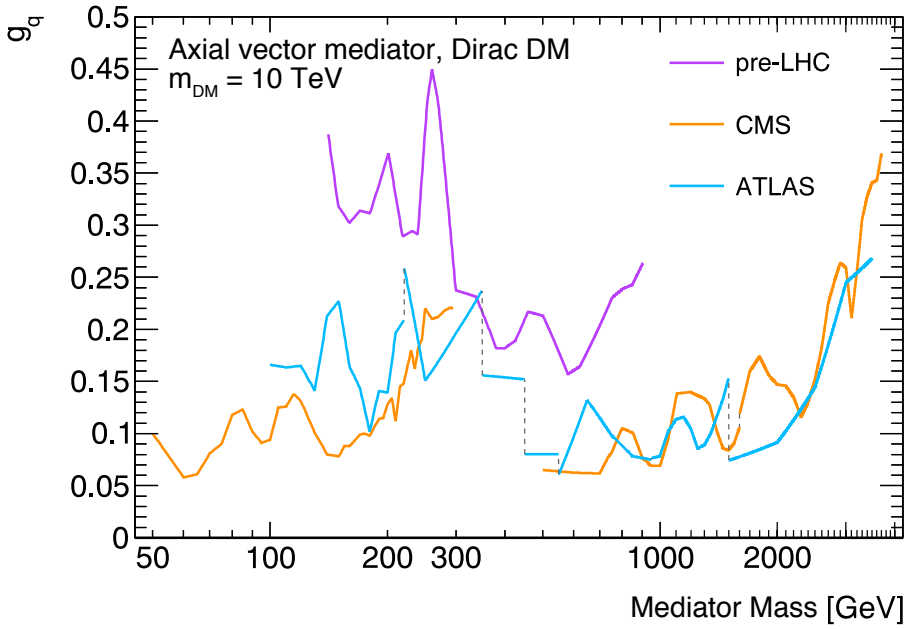

Figure 4

Summary of constraints from searches for light dijet resonances from ATLAS and CMS, where discrete points are taken from the coupling-mass limits on a simplified model mediated by an axial-vector Z' coupling exclusively to quarks from the searches mentioned in the text, and interpolated at the crossings. Couplings above the lines are excluded at 95% CL, up to the values where larger couplings yield a resonance width larger than 15% (roughly $g_q > 0.5$). Pre-LHC constraints have been taken from (142).

channel constrains g_q >0.15-0.2. Above 400 GeV, where searches with jets at the trigger level become available, they are the most sensitive, excluding g_q as low as 0.05. Above a TeV, standard dijet resonance and angular searches constrain quark couplings from 0.1 to unity, up to 5 TeV.

Mixing between this mediator and the Z boson induces loop-level couplings to leptons. ATLAS and CMS use several sets of coupling benchmarks to illustrate how the experimental constraints depend on these unknown values. For equal couplings of the mediator to leptons and jets, dilepton searches at a given mediator mass are far more sensitive than dijet searches. Other values will be discussed further in the next section.

3.5.1. Comparison of sensitivity of visible and invisible LHC searches. Fully-visible signatures of a particular dark interaction can be powerful probes of it, and in some cases (e.g., when the invisible particles are too heavy to be directly produced) are the only way to observe dark interactions at a collider. On the other hand, only $\not{E}_T$ searches can observe the invisible particle production directly. Each type of search complements the others; nevertheless, piecing together searches in different channels requires a model. Understanding precisely how these searches fit together can be challenging when the model is uncertain.

As an example, we again consider the case of vector or axial-vector mediators, to which both jet+$\not{E}_T$ and two-body resonance searches are sensitive. Though these models are

simple, their parameter space is four-dimensional (two couplings, the invisible particlemass, and the mediator mass). Recent ATLAS and CMS results depict their results in a two-dimensional plane of mediator mass and DM mass, following the recommendations of the LHC Dark Matter Working Group[4]. Figure shows a sampling of recent ATLAS plots. The other remaining coupling parameters are fixed to one of several benchmark sets, sets selected based on the sensitivity of early Run-2 searches, on precision constraints, and on the complementarity of different types of searches. The constraints from dijet, dilepton, and $\not{E}_T$ +X searches on the interaction model are displayed as excluded regions of the model parameter space.

The left plot in the figure shows the constraints for couplings g_q =0.25, g_l =0. and g_χ =1. In this case, dijet searches exclude mediators between about 200 GeV and 2.6 TeV, while $\not{E}_T$ +X searches can constrain even lighter mediators. The right plot shows the exclusions for smaller quark couplings, g_q of 0.1, and a non-zero lepton coupling, g_l of 0.01, chosen as indicative of the possible size of loop-induced lepton couplings. With lower quark couplings, and thus lower dijet production and decay rates, the regions of masses excluded by the several dijet searches shrink. For mediators heavier than 150 GeV, the exclusions from the recent dilepton search fare better but do not extend much into the (smaller) region excluded by the jet+$\not{E}_T$ search, where mediator decays to DM dominate.

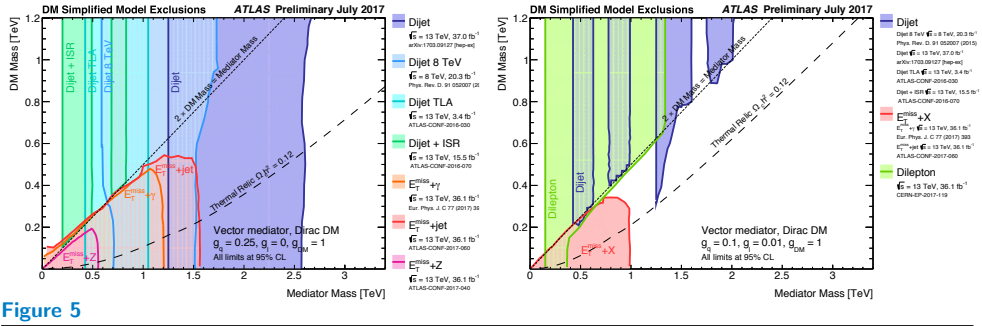

Figure 5

Regions in dark matter mass–Z′ mediator mass excluded at 95% CL by a selection of ATLAS dark matter searches for two coupling scenarios. Dashed curves labeled "thermal relic" indicate combinations of dark matter and mediator mass that are consistent with a dark matter density of $\omega_c = 0.12h^2$ and a standard thermal history, as computed in MadDM for this model (152). The dotted curve indicates the kinematic threshold where the mediator can decay on-shell into dark matter. From (153).

Thus, the relative sensitivity of visible and invisible searches is a model- and coupling-dependent statement. One advantage of searches for invisible particles over the others is their sensitivity to models with very light mediators (<50 GeV) and light m_χ, since the reach of dijet and dilepton searches to low-mass resonances is still ultimately limited by data taking constraints.

[4] akin to simplified models of SUSY, where the axes are neutralino mass and superpartner particle mass

4. EXTRAPOLATION OF COLLIDER RESULTS

A wide variety of reactions may produce invisible particles at colliders, and, if the mediators of the interaction are light enough to be produced on-shell, collider experiments are particularly suited to discovering and characterizing the interactions responsible. Meanwhile, connecting a collider experiment's discovery or non-discovery of invisible particles to dark matter requires direct and indirect detection experiments, where galactic dark matter collides with a terrestrial target, or extragalactic dark matter annihilates.

Making this connection requires that one assumes a particle physics model. Within a given model and under well-specified assumptions, the information obtained in a collider experiment can be related to the information obtained in direct, indirect, and astrophysical probes, and vice versa. One can then compare and contrast the different types of information, e.g., to understand where a DM discovery in current DD searches could be further explored with mediator studies at the LHC, and where, amongst the multitude of possible signals, collider searches might focus effort.

In the following, we outline a strategy adopted by the ATLAS and CMS experiments when making comparisons with astrophysical observations (e.g., where is a model consistent with the present DM density in the universe), DD, and ID results. We discuss the assumptions made in the relic density calculation and in relating reactions for invisible particles to reactions of DM.

4.1. Comparing LHC constraints from visible and invisible searches with non-collider results

The ATLAS and CMS collider results typically appear as constraints on production cross sections of specific processes, which are then interpreted as statements about the fundamental parameters of a simplified model (masses, couplings), Within the model, information on the parameters can then be extrapolated to statements about the non-collider observable of interest—for example, the WIMP-nucleon scattering cross section for DD, or the thermal relic density. In Ref. (30), the LHC Dark Matter Working Group provides an in-depth discussion of how to perform these extrapolations. Recently, most general LHC search results have selected a single, specific set of BSM-mediated simplified models for extrapolation, due to their immediate relevance with the first 13 TeV collision data. But many other models can be used [5], and published searches typically provide some form of model-agnostic results for this purpose.

As an example, CMS has extrapolated the parameter exclusions obtained by a recent set of searches to the spin-independent WIMP-nucleon cross section of a direct detection experiment. The result, Fig. 6, with a selection of DD results also shown for comparison, illustrates some general features of many such comparisons. For spin-independent scattering, LHC searches for heavy invisible particles are generally in the position of confirming non-observation of DM in DD searches, whereas LHC invisible particle searches are sensitive to arbitrarily light invisible particles while DD searches are not, and at intermediate DM masses both LHC and DD experiments have great potential for a discovery and could verify each other's claims. For spin-dependent DD scattering (e.g., an axial-vector-mediated model), because the LHC signals are relatively insensitive to the Lorentz structure of the

[5]For reinterpretation of LHC results and their comparisons to DD and ID for scalar and pseudoscalar mediators, also in the context of 2HDM, see e.g. (154, 155, 33)

The LHC Dark Matter Working Group: provides for the translation of LHC limits to DD and ID in (30), as well as calculations of relic density at `https://gitlab.cern.ch/lhc-dmwg-material/relic-density`.

interaction while the DD signals are suppressed, similar plots show that LHC searches play a more powerful role relative to the DD searches over a wide range of invisible particle masses.

In the same way, one can compare collider and ID results using simplified model benchmarks. In traditional comparisons, only one DM annihilation state at a time has been used for the comparison of collider and ID results (e.g. $b\bar{b}$, see for example (100)) but one can also compare ID and LHC results for models annihilating to multiple final state fermions. (156).

Recently, some DD and ID collaborations have adopted the benchmark simplified models being used by ATLAS and CMS, see e.g.(157, 158). IceCube and other experiments have used constraints from a MSSM scan, see e.g. (159). The pMSSM is also a good framework to highlight the complementarity of LHC, direct and indirect detection experiments, as shown in e.g. Ref, (160) and discussed later.

It must be underlined that the exclusion regions obtained in this way will depend strongly on the assumption of the model. The extrapolations are done with full knowledge that the simplified model is merely a crude guess, and one must be careful not to over-generalize. More so, neither this procedure nor the simplified models themselves account for effects outside the model, such as interference and mixing with SM boson and quarkonia resonances, or the evolution of the operators in the model from the LHC collision energies to other energy scales (161). Moreover, all experimental results, be it from DD, ID or collider, are affected by experimental and theoretical uncertainties that are not displayed here.

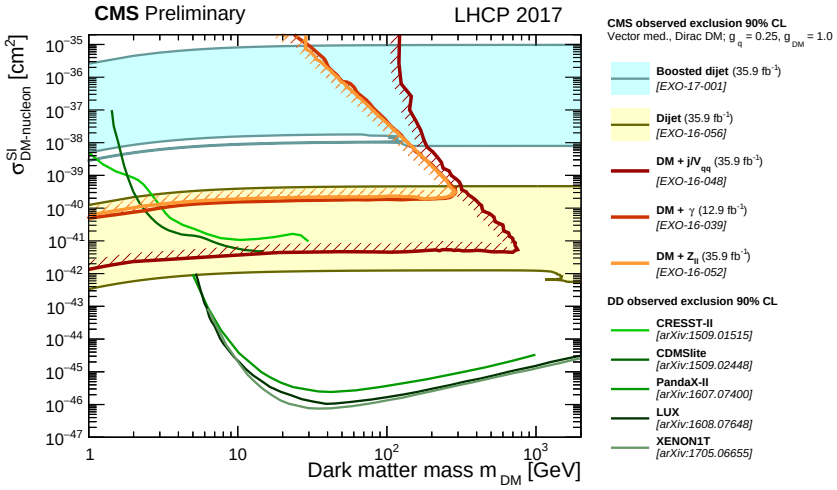

Figure 6

The 90% CL constraints from the CMS experiment in the m_χ-spin-independent DM-nucleon plane, for a vector mediator, Dirac DM and couplings $g_q = 0.25$ and $g_\chi = 1.0$, compared with DD experiments. From (162).

4.2. Relic density considerations

Absent a signal in non-collider experiments, the ability of a model to link its invisible particles with the observed DM abundance is key to distinguishing it from other types of models of physics beyond the Standard Model. Making this link, however, requires extrapolating from the present day to the early universe along an increasingly tenuous chain of assumptions. For simplified models, this is especially problematic, because the model is designed to describe collider-scale processes; it may not even contain the interactions relevant in the early universe. Nevertheless, it is interesting to examine where a model can make the link, even if in limited situations (163, 164). For example, for the general simplified models in Sec. 2.2.2, one can compute with programs such as MadDM and MicrOMEGas (152, 165) the DM abundance for a standard thermal relic assuming that the interaction described by the simplified model is the one responsible for setting the relic density. Often, e.g. Fig. 5, ATLAS and CMS supplement their results with contours indicating where within a model this procedure obtains the correct dark matter density of $\omega_c = 0.12h^2$. Where the model cannot reproduce the correct abundance, it is an indication that either the model requires additional ingredients beyond those included in the simplified model, or that the chain of assumptions is incorrect (6).

5. FUTURE EVOLUTION OF COLLIDER SEARCHES AND CONCLUSIONS

Here we highlight some topics to watch in the coming decade of dark matter searches at colliders.

FUTURE ISSUES

1. The obvious directions for LHC searches are towards lower-rate processes and processes that are more difficult to detect.
    - For such processes, extended scalar sectors and electroweak SUSY are among possible benchmarks. As Run-2 progresses, LHC searches are becoming sensitive to the simplest (pseudo-)scalar simplified models, opening the door to more realistic models. On a longer timescale, the HL-LHC dataset will bring sensitivity to up to 3 TeV in scalar mediator masses for unit couplings (166) and precision knowledge of the SM Higgs sector, e.g. at the level of 10, and the mass reach for electroweak production of SUSY partners increases by a few hundred GeV (167).
    - With data arriving at a slightly less frantic pace, experimentally challenging long-lived particle signatures are a growing field, and benchmarks similar to Ref. (8) are needed to help guide the design of these searches. Among many ongoing efforts, we note the bottom-up approach adopted in Ref. (168), which connects such models with the long-lived-particle limit of those in Chapter 2.2.2.
2. Precision searchers and efficient triggering of rare signals buried in large backgrounds are key to fully exploiting the HL-LHC dataset. LHCb will make use of a novel triggerless detector readout to perform dark photon searches at unprecedented sensitivities (169). These sorts of efforts should inspire ATLAS and CMS to

search for rare processes involving relatively light new particles, a subject they've left largely unexplored (170). In the familiar jet+$\not{E}_T$ search, precision estimates of the V+jet backgrounds, and of the inputs to these predictions, will be crucial. Efforts are ongoing in that direction (171).

3. Future hadron and electron-positron colliders have immense potential (see e.g. the studies towards a Future Hadron Collider (172)). Nevertheless, present studies largely continue the approaches already in use at the LHC. A new hadron collider would be built to discover new physics, and therefore qualitatively different experimental design, benchmark models, and analysis strategies should be considered.
4. More useful working comparisons between results from colliders, underground searches, and observatories should take into account the uncertainties on each type of result, and on the extrapolations between them. The main uncertainties for LHC searches have been outlined in Sec. 3 and in the experimental references. For a summary of DD and ID uncertainties, see Ref. (173, 174) and references therein.
5. Comparisons among collider and non-collider particle physics experiments are becoming standard, relating particle physics to astrophysical observables is crucial to exploit the few clues that dark matter can provide about particle physics beyond the SM. We highly encourage further work on this subject, e.g. Ref (175)

We are optimistic that, from collider approaches to underground experiments to observatories, the variety of powerful searches for particle dark matter will make much progress toward its discovery in the next decade. At colliders, the tools essential to discovering and understanding the fundamental particles of the Standard Model are once again being applied. Our understanding of collider search targets is also rapidly improving. Along with SUSY benchmarks motivated by the hierarchy problem, targets directly motivated by DM observations are encouraging a new generation of experimentalists to branch out into directions that so far are sparsely explored. Finally, the LHC is just at the beginning to take data at a new 13 TeV collision energy, with the goal of a dataset that exceeds that presented here by a factor of 100. These are exciting times.

DISCLOSURE STATEMENT

The authors are not aware of any affiliations, memberships, funding, or financial holdings that might be perceived as affecting the objectivity of this review.

ACKNOWLEDGMENTS

We thank William Kalderon, Teng Jian Khoo, Suchita Kulkarni, Priscilla Pani, and Frederik Ruehr for their help and advice in preparing this manuscript. We also thank Ulrich Haisch, Valerio Ippolito, Christian Ohm, Jessie Shelton, and Mike Williams for useful discussion. Work by AB is supported by the US Department of Energy (Grant DE-SC0011726). Work by CD is part of a project that has received funding from the European Research Council (ERC) under the European Union's Horizon 2020 research and innovation programme (Grant Agreement No. 679305) and from the Swedish Research Council.

LITERATURE CITED

1. Bertone G, Hooper D. *Submitted to: Rev. Mod. Phys.* (2016)
2. Steigman G. *Ann. Rev. Nucl. Part. Sci.* 29:313 (1979)
3. Ade PAR, et al. *Astron. Astrophys.* 594:A13 (2016)
4. Undagoitia TM, Rauch L. *Journal of Physics G: Nuclear and Particle Physics* 43:013001 (2016)
5. Gaskins JM. *Contemp. Phys.* 57:496 (2016)
6. Bernal N, et al. *Int. J. Mod. Phys.* A32:1730023 (2017)
7. D'Ambrosio G, Giudice GF, Isidori G, Strumia A. *Nucl. Phys.* B645:155 (2002)
8. Abercrombie D, et al. arXiv:1507.00966 [hep-ex] (2015)
9. Escudero M, Berlin A, Hooper D, Lin MX. *JCAP* 1612:029 (2016)
10. Patt B, Wilczek F arXiv:hep-ph/0605188 [hep-ph] (2006)
11. Djouadi A, Lebedev O, Mambrini Y, Quevillon J. *Phys. Lett.* B709:65 (2012)
12. Goodman J, et al. *Phys.Rev.* D82:116010 (2010)
13. Bai Y, Fox PJ, Harnik R. *JHEP* 1012:048 (2010)
14. Fox PJ, Harnik R, Kopp J, Tsai Y. *Phys. Rev.* D85:056011 (2012)
15. Shoemaker IM, Vecchi L. *Phys.Rev.* D86:015023 (2012)
16. Racco D, Wulzer A, Zwirner F. *JHEP* 1505:009 (2015)
17. Busoni G, De Simone A, Morgante E, Riotto A. *Phys.Lett.* B728:412 (2014)
18. Alwall J, Schuster P, Toro N. *Phys. Rev.* D79:075020 (2009)
19. LHC New Physics Working Group. *J. Phys.* G39:105005 (2012)
20. Abdallah J, et al. *Phys. Dark Univ.* 9-10:8 (2015)
21. Kahlhoefer F, Schmidt-Hoberg K, Schwetz T, Vogl S. *JHEP* 02:016 (2016)
22. Backovic M, et al. *Eur. Phys. J.* C75:482 (2015)
23. Papucci M, Vichi A, Zurek KM. *JHEP* 1411:024 (2014)
24. An H, Wang LT, Zhang H. *Phys.Rev.* D89:115014 (2014)
25. Bell NF, et al. *Phys.Rev.* D86:096011 (2012)
26. Han C, Lee HM, Park M, Sanz V. *Phys. Lett.* B755:371 (2016)
27. Albert A, et al. arXiv:1703.05703 [hep-ex] (2017)
28. Berlin A, Lin T, Wang LT. *JHEP* 1406:078 (2014)
29. Chala M, et al. arXiv:1503.05916 [hep-ph] (2015)
30. Boveia A, et al. arXiv:1603.04156 [hep-ex] (2016)
31. Buckley MR, Feld D, Goncalves D. *Phys.Rev.* D91:015017 (2015)
32. Haisch U, Re E. *JHEP* 1506:078 (2015)
33. Bell NF, Busoni G, Sanderson IW. *JCAP* 1703:015 (2017)

34. Albert A, et al. *Phys. Dark Univ.* 16:49 (2017)
35. Englert C, McCullough M, Spannowsky M. *Phys. Dark Univ.* 14:48 (2016)
36. Bai Y, Berger J. *JHEP* 11:171 (2013)
37. Ko P, Natale A, Park M, Yokoya H. *JHEP* 01:086 (2017)
38. Buschmann M, et al. *JHEP* 09:033 (2016)
39. Khoze VV, Plascencia AD, Sakurai K. *JHEP* 06:041 (2017)
40. Ellis JR, Falk T, Olive KA, Srednicki M. *Astropart. Phys.* 13:181 (2000), [Erratum: Astropart. Phys.15,413(2001)]
41. Blanke M, Kast S. *JHEP* 05:162 (2017)
42. Boucheneb I, Cacciapaglia G, Deandrea A, Fuks B. *JHEP* 01:017 (2015)
43. Duerr M, et al. *JHEP* 09:042 (2016)
44. Bauer M, Haisch U, Kahlhoefer F. *JHEP* 05:138 (2017)
45. Goncalves D, Machado PAN, No JM. *Phys. Rev.* D95:055027 (2017)
46. Feng JL. *Ann. Rev. Astron. Astrophys.* 48:495 (2010)
47. Ellis J, et al. *Nuclear Physics B* 238:453 (1984)
48. Farrar GR, Fayet P. *Phys. Lett.* 76B:575 (1978)
49. Dimopoulos S, Dine M, Raby S, Thomas SD. *Phys. Rev. Lett.* 76:3494 (1996)
50. Masiero A, Profumo S, Ullio P. *Nucl. Phys.* B712:86 (2005)
51. Pospelov M, Ritz A, Voloshin MB. *Phys. Lett.* B662:53 (2008)
52. Das S, Sigurdson K. *Phys. Rev.* D85:063510 (2012)
53. Co RT, D'Eramo F, Hall LJ, Pappadopulo D. *JCAP* 1512:024 (2015)
54. Holdom B. *Phys. Lett.* 166B:196 (1986)
55. Curtin D, Essig R, Gori S, Shelton J. *JHEP* 02:157 (2015)
56. Battaglieri M, et al. arXiv:1707.04591 [hep-ph] (2017)
57. El Hedri S, Kaminska A, de Vries M, Zurita J. *JHEP* 04:118 (2017)
58. Strassler MJ, Zurek KM. *Phys. Lett.* B651:374 (2007)
59. Evans JA, Gori S, Shelton J arXiv:1712.03974 [hep-ph] (2017)
60. Zurek KM. *Phys. Rept.* 537:91 (2014)
61. Craig N, Knapen S, Longhi P. *Phys. Rev. Lett.* 114:061803 (2015)
62. Evans L, Bryant P. *JINST* 3:S08001 (2008)
63. ATLAS Collaboration. *JINST* 3:S08003 (2008)
64. CMS Collaboration. *JINST* 3:S08004 (2008)
65. LHCb Collaboration. *JINST* 3:S08005 (2008)
66. Schael S, et al. *Phys. Rept.* 427:257 (2006)
67. Carena M, de Gouvea A, Freitas A, Schmitt M. *Phys. Rev.* D68:113007 (2003)
68. ATLAS Collaboration. *Eur. Phys. J.* C77:765 (2017)
69. ATLAS and CMS Collaborations. *JHEP* 08:045 (2016)
70. ATLAS Collaboration. *JHEP* 11:206 (2015)
71. Dobrescu BA, Lykken JD. *JHEP* 02:073 (2013)
72. CMS Collaboration. *JHEP* 02:135 (2017)
73. ATLAS Collaboration. *Eur. Phys. J.* C77:241 (2017)
74. CMS Collaboration. *CMS-PAS-JME-16-004* (2016)
75. ATLAS Collaboration. *ATLAS-CONF-2014-019* (2014)
76. ATLAS Collaboration. *ATLAS-CONF-2015-029* (2015)
77. ATLAS Collaboration. *Phys. Rev.* D94:032005 (2016)
78. Fox PJ, Harnik R, Kopp J, Tsai Y. *Phys.Rev.* D84:014028 (2011)
79. Haisch U, Kahlhoefer F, Re E. *JHEP* 1312:007 (2013)
80. Smith WH. *Ann. Rev. Nucl. Part. Sci.* 66:123 (2016)
81. ATLAS Collaboration arXiv:1711.03301 [hep-ex] (2017)
82. CMS Collaboration arXiv:1712.02345 [hep-ex] (2017)
83. Lindert JM, et al. *Eur. Phys. J.* C77:829 (2017)

84. Maguire E, Heinrich L, Watt G. *J. Phys. Conf. Ser.* 898:102006 (2017)
85. CMS Collaboration (2017)
86. CMS Collaboration arXiv:1711.00431 [hep-ex] (2017)
87. ATLAS Collaboration. *Phys. Lett.* B776:318 (2018)
88. Birkedal A, Matchev K, Perelstein M. *Phys.Rev.* D70:077701 (2004)
89. Carpenter LM, et al. *Phys. Rev.* D87:074005 (2013)
90. ATLAS Collaboration. *Eur. Phys. J.* C77:393 (2017)
91. CMS Collaboration. *CMS-PAS-EXO-16-014* (2016)
92. ATLAS Collaboration. *Phys. Lett.* B763:251 (2016)
93. Larkoski AJ, Moult I, Nachman B arXiv:1709.04464 [hep-ph] (2017)
94. CMS Collaboration. *CMS-PAS-EXO-16-054* (2017)
95. ATLAS Collaboration. *Phys. Rev.* D96:112004 (2017)
96. ATLAS Collaboration. *Phys. Rev. Lett.* 119:181804 (2017)
97. ATLAS Collaboration arXiv:1710.11412 [hep-ex] (2017)
98. ATLAS Collaboration arXiv:1711.11520 [hep-ex] (2017)
99. CMS Collaboration arXiv:1711.00752 [hep-ex] (2017)
100. Agrawal P, Batell B, Hooper D, Lin T. *Phys.Rev.* D90:063512 (2014)
101. CMS Collaboration arXiv:1801.08427 [hep-ex] (2018)
102. ATLAS Collaboration. *Eur. Phys. J.* C75:79 (2015)
103. Lester CG, Summers DJ. *Phys. Lett.* B463:99 (1999)
104. ATLAS Collaboration. *Phys. Rev.* D96:112010 (2017)
105. CMS Collaboration. *JHEP* 12:142 (2017)
106. CMS Collaboration. *JHEP* 10:005 (2017)
107. ATLAS Collaboration. *JHEP* 09:175 (2016)
108. ATLAS Collaboration. Supersymmetry Public Results (2018), `https://twiki.cern.ch/twiki/bin/view/AtlasPublic/SupersymmetryPublicResults`
109. CMS Collaboration. Supersymmetry Public Results (2018), `https://twiki.cern.ch/twiki/bin/view/CMSPublic/PhysicsResultsSUS`
110. CMS Collaboration arXiv:1801.03957 [hep-ex] (2018)
111. ATLAS Collaboration. *ATLAS-CONF-2017-039* (2017)
112. ATLAS Collaboration arXiv:1712.08119 [hep-ex] (2017)
113. CMS Collaboration. *JHEP* 11:029 (2017)
114. ATLAS Collaboration (2017)
115. CMS Collaboration arXiv:1802.02110 [hep-ex] (2018)
116. Conley JA, et al. *Eur. Phys. J.* C71:1697 (2011)
117. ATLAS Collaboration. *JHEP* 10:134 (2015)
118. CMS Collaboration. *JHEP* 10:129 (2016)
119. Athron P, et al. *Eur. Phys. J.* C77:784 (2017)
120. Bagnaschi E, et al. arXiv:1710.11091 [hep-ph] (2017)
121. ATLAS Collaboration arXiv:1712.02118 [hep-ex] (2017)
122. CMS Collaboration. *JHEP* 01:096 (2015)
123. Ball A, et al. arXiv:1607.04669 [physics.ins-det] (2016)
124. Chou JP, Curtin D, Lubatti HJ. *Phys. Lett.* B767:29 (2017)
125. LHCb Collaboration arXiv:1710.02867 [hep-ex] (2017)
126. LHCb Collaboration. *Comput. Phys. Commun.* 208:35 (2016)
127. BaBar Collaboration. *Phys. Rev. Lett.* 113:201801 (2014)
128. Lees JP, et al. *Phys. Rev. Lett.* 119:131804 (2017)
129. LHCb Collaboration. *Phys. Rev.* D95:071101 (2017)
130. ATLAS Collaboration. *ATLAS-CONF-2016-042* (2016)
131. CMS Collaboration. *CMS-PAS-HIG-16-035* (2016)
132. Liew SP, Papucci M, Vichi A, Zurek KM. *JHEP* 06:082 (2017)

133. ATLAS Collaboration. *Phys. Rev.* D96:052004 (2017)
134. CMS Collaboration. *CMS-PAS-EXO-16-056* (2017)
135. CMS Collaboration. *CMS-PAS-EXO-16-046* (2017)
136. ATLAS Collaboration. *Eur. Phys. J.* C77:317 (2017)
137. CMS Collaboration. *JINST* 12:P01020 (2017)
138. CMS Collaboration. *CMS-PAS-JME-14-001* (2014)
139. ATLAS Collaboration. *CERN-LHCC-2013-007, ATLAS-TDR-021* (2013)
140. CMS Collaboration. *JINST* 6:C12065 (2011)
141. An H, Huo R, Wang LT. *Phys. Dark Univ.* 2:50 (2013)
142. Dobrescu BA, Yu F. *Phys. Rev.* D88:035021 (2013), [Erratum: Phys. Rev.D90,no.7,079901(2014)]
143. ATLAS Collaboration. *ATLAS-CONF-2016-030* (2016)
144. ATLAS Collaboration. *ATLAS-CONF-2016-070* (2016)
145. CMS Collaboration arXiv:1710.00159 [hep-ex] (2017)
146. Aaboud M, et al. arXiv:1801.08769 [hep-ex] (2018)
147. ATLAS Collaboration. *ATLAS-CONF-2016-031* (2016)
148. CMS Collaboration. *CMS-PAS-HIG-16-025* (2016)
149. ATLAS Collaboration. *Phys. Rev. Lett.* 119:191803 (2017)
150. ATLAS Collaboration. *JHEP* 10:182 (2017)
151. CMS Collaboration. *Phys. Lett.* B768:57 (2017)
152. Backovic M, et al. *Phys. Dark Univ.* 9-10:37 (2015)
153. ATLAS Collaboration. Summary plots from the ATLAS Exotic physics group (2017), `https://atlas.web.cern.ch/Atlas/GROUPS/PHYSICS/CombinedSummaryPlots/EXOTICS/index.html#ATLAS_DarkMatter_Summary`
154. GAMBIT Collaboration. *Eur. Phys. J.* C77:568 (2017)
155. Banerjee S, et al. *JHEP* 07:080 (2017)
156. Carpenter LM, Colburn R, Goodman J, Linden T. *Phys. Rev.* D94:055027 (2016)
157. Collaboration P. *Phys. Rev. Lett.* 118:251301 (2017)
158. Balazs C, et al. *Phys. Rev.* D96:083002 (2017)
159. Aartsen MG, et al. *Eur. Phys. J.* C77:146 (2017)
160. Cahill-Rowley M, Hewett JL, Ismail A, Rizzo TG. *Phys. Rev.* D91:055002 (2015)
161. D'Eramo F, Procura M. *JHEP* 04:054 (2015)
162. CMS Collaboration. Dark Matter Summary Plots from CMS for LHCP and EPS 2017 (2017), `https://twiki.cern.ch/twiki/pub/CMSPublic/PhysicsResultsEXO/DM-summary-plots-Jul17.pdf`
163. Busoni G, et al. *JCAP* 1503:022 (2015)
164. Catena R, Conrad J, Krauss MB arXiv:1712.07969 [hep-ph] (2017)
165. Barducci D, et al. *Comput. Phys. Commun.* 222:327 (2018)
166. Estimated Sensitivity for New Particle Searches at the HL-LHC. Tech. Rep. CMS-PAS-FTR-16-005, CERN, Geneva (2017)
167. Campana P, Klute M, Wells P. *Ann. Rev. Nucl. Part. Sci.* 66:273 (2016)
168. Buchmueller O, et al. *JHEP* 09:076 (2017)
169. Ilten P, et al. *Phys. Rev. Lett.* 116:251803 (2016)
170. Alves A, et al. *JHEP* 04:164 (2017)
171. Blumenschein U, et al. arXiv:1802.02100 [hep-ex] (2018)
172. Golling T, et al. *CERN Yellow Report* :441 (2017)
173. Feldstein B, Kahlhoefer F. *JCAP* 1412:052 (2014)
174. Auchettl K, Balazs C. In-Tech (2012)
175. Buckley MR, Peter AHG arXiv:1712.06615 [astro-ph.CO] (2017)

RELATED RESOURCES

G. Bertone *et al.*, Particle Dark Matter: Observations, Models and Searches *Cambridge: Cambridge Univ. Press* (2010),

Bertone G, Hooper D. A History of Dark Matter *Submitted to: Rev. Mod. Phys.* (2016)

Plehn T. Yet Another Introduction To Dark Matter (2017), `http://www.thphys.uni-heidelberg.de/~plehn/pics/dark_matter.pdf`

G. Arcadi, M. Dutra, P. Ghosh, M. Lindner, *et al.* The Waning of the WIMP? A Review of Models, Searches, and Constraints *arXiv:1703.07364 [hep-ph].*

F. Kahlhoefer, Review of LHC Dark Matter Searches *arXiv:1702.02430 [hep-ph], Int. J. Mod. Phys. A* **32**, *no. 13, 1730006 (2017)*

LHC Physics Centre Working Group on Dark Matter Searches at the LHC (2015-), `http://lpcc.web.cern.ch/content/lhc-dm-wg-wg-dark-matter-searches-lhc`